Plasma Chem Plasma Process (2013) 33:1083–1098
DOI 10.1007/s11090-013-9487-z

ORIGINAL PAPER

Ozone-Assisted Catalysis of Toluene with Layered ZSM-5 and Ag/ZSM-5 Zeolites

Hyun-Ha Kim · Masami Sugasawa · Hiroshi Hirata · Yoshiyuki Teramoto · Katsunori Kosuge · Nobuaki Negishi · Atsushi Ogata

Received: 2 July 2013 / Accepted: 2 September 2013 / Published online: 21 September 2013
© Springer Science+Business Media New York 2013

Abstract This paper presents a new type of ozone-assisted catalysis for toluene decomposition. The different catalytic activities of ZSM-5 and Ag/ZSM-5 were incorporated into a layered catalyst with a tandem configuration. Instead of increasing the amount of metal catalyst, the layered catalyst was formed, which had an equal amount of bare ZSM-5 and Ag/ZSM-5 and could achieve both high toluene conversion and CO_2 selectivity concurrently. The properties of each catalyst were evaluated with respect to toluene conversion, formation of intermediates, CO_2 selectivity and ozone demand factor. The bare ZSM-5 exhibited higher toluene conversion than the Ag/ZSM-5, while its activity toward deep oxidation was limited. However, the Ag/ZSM-5 was found to be effective for the deep oxidation of reaction intermediates (HCOOH and CO). Separate oxidation tests with HCOOH and CO revealed that the ZSM-5-supported Ag nanoparticles could oxidize the HCOOH and CO in the absence of ozone, which was not possible with the bare ZSM-5. Plausible pathways for the oxidation of toluene with O_3 over ZSM-5 and Ag/ZSM-5 were proposed based on the experimental evidence.

Keywords Ozone-assisted catalysis · VOC · Layered catalyst · Ag/ZSM-5

Introduction

Volatile organic compounds (VOCs) have been a subject of environmental and public health concern because they substantially contribute to photochemical oxidants and secondary organic aerosols. In 2006 in Japan, air pollution control laws have severely restricted the emission of VOCs from large plant facilities used for the painting, drying, cleaning, printing, and storage industries. Conventional pollution control methods,

H.-H. Kim (✉) · M. Sugasawa · H. Hirata · Y. Teramoto · K. Kosuge · N. Negishi · A. Ogata
Research Institute for Environmental Management Technology, National Institute of Advanced Industrial Science and Technology (AIST), 16-1 Onogawa, Tsukuba 305-8569, Japan
e-mail: hyun-ha.kim@aist.go.jp

including incineration, catalytic combustion and adsorption techniques, have already been implemented at large exhaust sources [1–3]. However, these techniques are unsuitable for many small- and medium-sized plant facilities because they are expensive and require a large space for installation. Therefore, more effective and inexpensive techniques must be developed for use in these small- and medium-sized plant facilities. Platinum-group metals, such as platinum and palladium, are currently used as active materials in catalysts. However, the use of these rare metals will most likely be restricted in the future because they are increasingly in demand for various applications, such as automobile catalysts, combustion catalysts, and fuel cell electrodes [4]. Some other transition metals exhibit catalytic activity, but these elements require higher reaction temperatures than are necessary with the platinum-group catalyst [5, 6].

The combination of electrical discharge with catalysis has become more popular for applications in VOC control because these processes yield higher conversion and superior CO_2 selectivity [7–9]. These combined systems fall into two basic categories; one is single-stage (also referred to as plasma-driven or in-plasma catalysis) and the other is two-stage (also referred to as plasma-assisted or post-plasma catalysis) [10, 11]. Precious metals (Pt, Pd) are also not essential for successful plasma-catalysis processes. Ozone (O_3)-assisted catalysis is one optimized type of the two-stage plasma-assisted catalysis because the plasma is specifically used for ozone generation. Previous studies have indicated that using ozone can reduce the reaction temperature by approximately 200 °C during the oxidations of CO and benzene (C_6H_6) over a blast furnace slag catalyst containing several metals (Cu, Ni, Mn, Co) [12], the oxidation of *i*-propanol and CO over $CoOx/Al_2O_3$ [13], and the oxidations of several VOCs over $Ba–CuO–Cr_2O_3/Al_2O_3$ [14]. One important feature of the ozone-assisted catalysis is the complete control over NOx formation, which is not possible with the other types of combined plasma-catalysis processes operating in air-like mixtures [9, 15, 16]. Ozone-assisted catalysis is essentially free from ion chemistry [17], short-lived radicals [18], UV [19], excited or metastable molecules [20, 21], and surface streamers [22, 23], which often make the interactions between the plasma and the catalyst in single-stage configuration difficult to understand.

Several authors have considered using multi-component catalysts to increase the performance in single-stage or two-stage plasma-catalysis processes. Ogata et al. [24] reported the combined effects of $BaTiO_3$ with metal-supported alumina, as well as $BaTiO_3$ with zeolites [25] on the decomposition of benzene. Holzer et al. [26] has also confirmed that enhanced performance in methyl *tert*-butyl ether (MTBE) destruction can be achieved with a packed-bed (single-stage) reactor containing both $BaTiO_3$ and $LaCoO_3$. A group at the University of Manchester reported the destruction of toluene and cyclohexane in air using a two-stage plasma-enhanced catalyst process. They used dual-layer catalysts composed of MnO_2/alumina and MnO_2-CuO downstream from the plasma cells [27]. Although the carbon balances were very low (below 25 %), which is most likely due to the adsorption of intermediates on the surface of catalysts, this configuration produced more CO_2 with less outlet O_3. A similar effect was also reported when a mixed catalyst, which was composed of MnO_2/TiO_2-Al_2O_3 and TiO_2, was used for the removal of toluene (750 ppbv) [28]. However, these approaches have not yet been studied for the ozone-assisted catalysis of VOCs. In this study, different catalytic activities from using ZSM-5 and Ag/ZSM-5 were incorporated into layered catalysts, in which the ZSM-5 was followed by the Ag/ZSM-5. Comparison of the new system with the individual catalysts, as well as the development of the optimum ratio for the layered catalyst, will be discussed. The screening of suitable catalysts, which include parameters such as the type of metal or support, is an important issue during the optimization of the O_3-assisted catalysis. The most widely studied

materials used in O_3-assisted catalysis are Mn oxides (MnO_x) [29–32]. Various metal oxides [33], titania-supported V_2O_5 [34], wood fly ash [35], and Cu–Cr catalysts [36, 37] have also been studied recently in low reaction temperatures (e.g., room temperature or 100 °C). Furthermore, porous materials, such as zeolites and MCM-41, have also been used as supports or even catalysts during oxidation reactions [31, 38, 39]. Sugasawa and Ogata [40] reported that ZSM-5-supported Ag (Ag/ZSM-5) decomposed toluene ($C_6H_5CH_3$) more efficiently than systems using Mn, Fe, Co, or Ni. We focused on the behavior of ZSM-5 and Ag/ZSM-5 during the oxidation of 200 ppm toluene using varying inlet O_3 concentrations, catalyst loadings, and reaction temperatures. The carbon recovery in a previously reported O_3-assisted catalytic oxidation of 100 ppm benzene (C_6H_6) was below 40 % at room temperature [41]. Formation of intermediates and their accumulation on the catalyst surface cause the low carbon recovery and deactivation of the catalyst over time [42]. Increasing the reaction temperature and the amount of catalyst are simple changes that may increase the carbon recovery [40] and decrease the outlet ozone (complete utilization of ozone). Temperature limit of ozone-assisted catalysis will be about 270 °C due to the rapid decomposition of O_3 in gas-phase. To elucidate the catalytic role of Ag in the deep oxidation, separate test oxidations using two major byproducts (100 ppm HCOOH and 160 ppm CO) were also conducted. A plausible reaction mechanism will be presented based on the experimental evidence.

Experimental Section

Catalyst Preparation

Hydrophobic ZSM-5 pellets (Union Showa K. K., Japan HiSiv-3000, diameter = 1.6 mm, Si/Al ratio >1,000) were impregnated with an aqueous solution of $AgNO_3$, before drying at 40 °C in a rotary evaporator, finally the material was calcined in air at 500 °C for 10 h. The amount of Ag (4.4 wt%) on the prepared catalyst (Ag/ZSM-5) was determined with inductively coupled plasma-atomic emission spectrometry (ICP-AES, SII Nano Technology Inc., Japan, Model SPS 5100). The Brunauer-Emmett-Teller (BET) surface area of the ZSM, which was determined via N_2 adsorption using BELSORP 28 system (BEL Japan) at liquid nitrogen temperature, decreased from 313 to 294 m^2/g after loading the Ag. The morphology and size of the Ag nanoparticles on the ZSM-5 zeolite were measured with a transmission electron microscope (TEM; Topcon EM-022B). Figure 1 presents a TEM image of Ag/ZSM-5. The Ag nanoparticles were uniformly dispersed on ZSM-5 (2–7 nm) with a mean particle size of approximately 3 nm. All catalysts were pretreated in dry air at 500 °C for 1 h before each test run. The oxidation state of the impregnated Ag was measured using X-ray diffractometer (Rigaku, Model MiniFlex II), which is shown in Fig. 2. Most of Ag peaks were ascribed to metallic Ag and the Ag oxide was found to be trace or negligible.

Experimental Apparatus

The experimental setup is described schematically in Fig. 3. An oxygen-fed (0.1 L/min) surface discharge type ozonizer was made of a quartz tube with an 11.5 mm outer diameter, a 9.5 mm inner diameter, and a length of 150 mm. The ozonizer was energized using an AC high voltage power supply (Trek JAPAN Co., Japan 20/20B). The discharge power (0.2–2.0 W) was measured using the Lissajous method [43]. The catalyst reactor

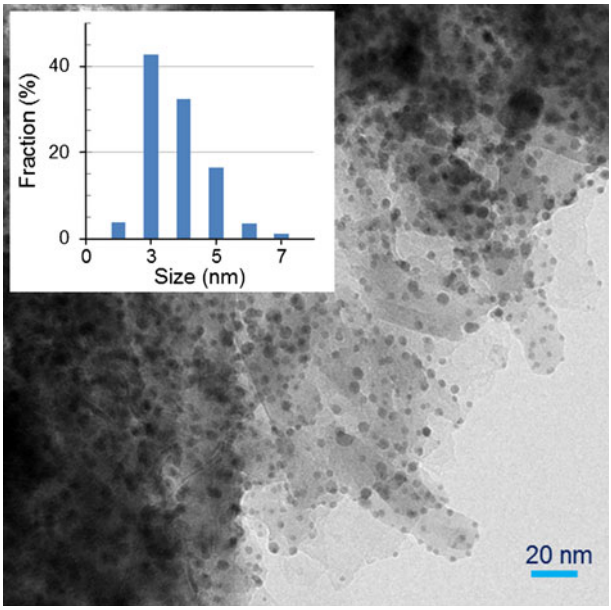

Fig. 1 TEM photograph of Ag/ZSM-5 with a magnification of 55,000

Fig. 2 XRD pattern of the Ag/ZSM-5

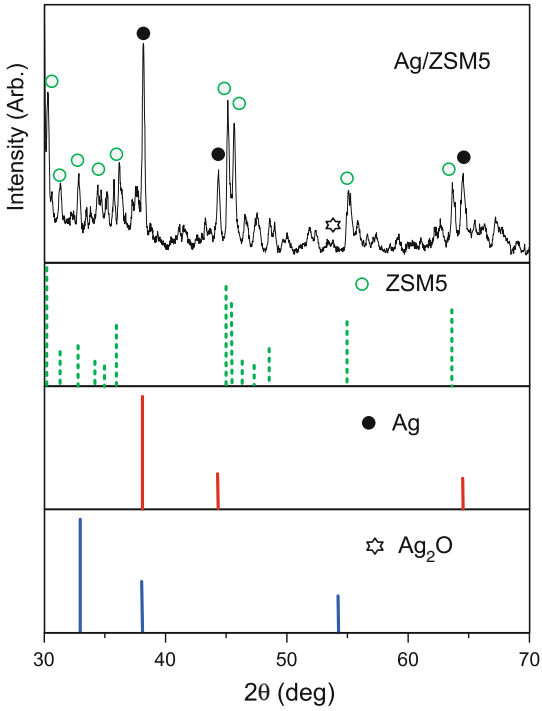

was made of a quartz tube with a 12.5 mm outer diameter, a 10.0 mm inner diameter, and a 210 mm length, which was placed vertically in an electrical oven. A glass bubbler containing liquid toluene placed in a water-bath, where the temperature was thermostatically-controlled at 5 °C. The toluene concentration was controlled either by the flow rate of the nitrogen through the bubbler or the temperature of water-bath. The flow rate of each gas was independently controlled with a mass flow controller (MFC). The toluene/N_2 gas (0.4 L/min) and the O_3/O_2 gas (0.1 L/min) were mixed upstream from the catalyst bed. As was expected from the small reaction rate constant ($k = -10^{-22}$ molecules/cm^3), no decomposition occurred when the O_3 was mixed with toluene at room temperature in the absence of catalyst. The inlet concentrations of toluene and O_3 were adjusted to 200 and 660–4,100 ppm, respectively. The O_3-assisted catalytic oxidation was begun after the toluene adsorption reached equilibrium.

In this study, four sets of experimental conditions were examined by varying the reaction temperature and amount of catalyst: (A) 0.5 g of catalyst at a reaction temperature of 100 °C, (B) 0.5 g of catalyst at 150 °C, (C) 1.0 g of catalyst at 100 °C, and (D) 1.0 g of catalyst at 150 °C. These four sets of experiments may provide important insight into optimal temperature and amount of catalyst. Gaining an understanding the formation and the further oxidation of two major intermediates (HCOOH and CO) is particularly important. The oxidation abilities of ZSM-5 and Ag/ZSM-5 for the conversion of HCOOH and CO were also examined to elucidate the catalytic properties during the toluene degradation. The concentrations of HCOOH and CO in the mixed gases (0.5 L/min) were 100 and 160 ppm, respectively.

The characteristics of each catalyst were incorporated into tandem layered catalysts, where ZSM-5 was followed by Ag/ZSM-5 in the direction of the gas flow (Fig. 3). The

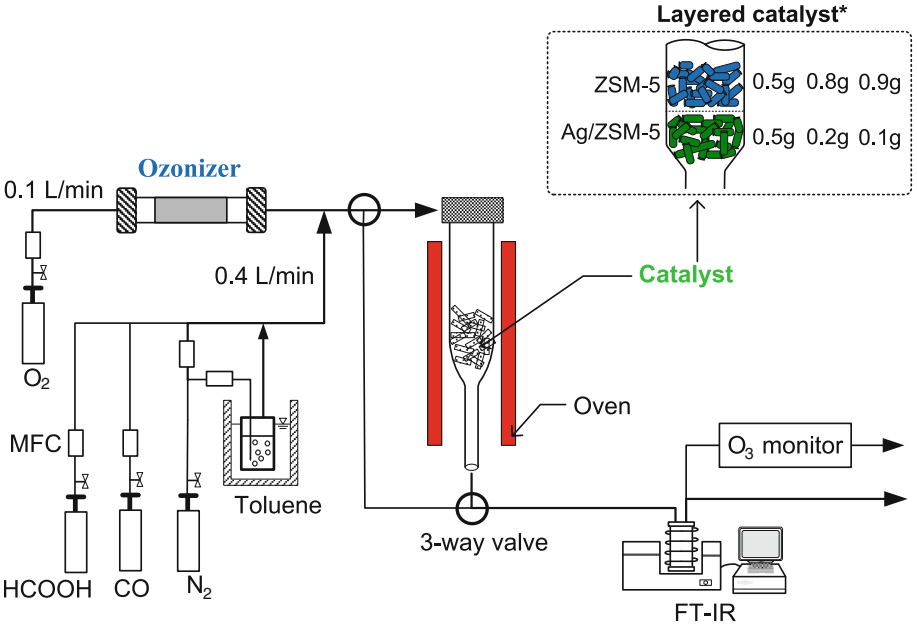

Fig. 3 Experimental setup for the ozone-assisted catalytic decomposition of toluene. Unless otherwise noted, the test conditions were as follows: *a* 0.5 g of catalyst at 100 °C, *b* 0.5 g of catalyst at 150 °C, *c* 1.0 g of catalyst at 100 °C, *d* 1.0 g of catalyst at 150 °C

total amount of layered catalyst was 1.0 g and different ratios of ZSM-5 and Ag/ZSM-5 were also surveyed. Glass filters were used to hold and to separate each catalyst bed. The reaction temperature was maintained at 100 or 150 °C by an electrical furnace, and the O_3 concentration was adjusted to 2,423 or 2,700 ppm.

Analysis

The concentrations of the toluene and the oxidation products (CO_2, CO, and HCOOH) were measured with an online Fourier transform infrared spectrometer (FT-IR, Jasco Co., Japan FT/IR-4200) equipped with a gas cell 2.5 m in optical length (Specac Inc., UK Sirocco series 24102). The spectral resolution of the FT-IR was set at 0.5 cm^{-1}. The concentrations of toluene, CO_2, CO, and HCOOH were determined quantitatively from the absorption peaks at 729.2, 2,296.3, 2,190.0, and 1,103.0 cm^{-1}, respectively. The concentration of O_3 was measured with an O_3 monitor (Ebara Jitsugyo Co., Japan EG-550) downstream from the FT-IR. The data points in this work represent the data read beginning 30 min after the start of O_3 supply to the catalyst reactor, unless otherwise noted. The toluene conversion and CO_2 selectivity were calculated with the following equations.

$$\text{Conversion}\,(\%) = \frac{[\text{Toluene}]_0 - [\text{Toluene}]}{[\text{Toluene}]_0} \times 100 \quad (1)$$

$$\text{CO}_2\ \text{selectivity}\,(\%) = \frac{[\text{CO}_2]}{[\text{CO}_2] + [\text{CO}] + [\text{CHOOH}]} \times 100 \quad (2)$$

The subscript 0 indicates the inlet concentration. The CO_2 selectivity in CO_x indicates the ratio of CO_2 from the sum of CO and CO_2.

Results and Discussion

Catalytic Activity of Bare ZSM-5

The toluene conversion over the bare ZSM-5 was plotted against the inlet the O_3 concentration in Fig. 4. As the temperature and the amount of catalyst increased, the conversion of toluene increased. Under all tested conditions (A, B, C, and D), the conversion of toluene and the formation of the oxidation products (CO, CO_2, and HCOOH) became progressively saturated when the inlet O_3 concentrations exceeded approximately 2,700 ppm. Figure 5 displays (a) the ozone consumption and (b) the concentrations of the oxidation products formed over the bare ZSM-5. The lowest ozone consumption was observed with condition A, which reflects the poor conversion of toluene (Fig. 3), the limited formation of oxidized products and the low CO_2 selectivity. This observation indicates that the decomposition of ozone generates active oxygen species on the bare ZSM-5, which leads to the oxidation of the toluene [44–46].

Figure 6 illustrates the (a) profiles of HCOOH, and (b) CO_2 selectivity. The HCOOH formation was noticeable at conditions A and C (100 °C). The peak values reached 124 and 131 ppm, respectively. Further increasing the amount of inlet O_3 to a concentration above 1,260 ppm resulted in the accumulation of less HCOOH. The declining slope was proportional to the amount of ZSM-5 (condition C > condition A), but detectable amounts of HCOOH still existed, even with 4,000 ppm of ozone. On the other hand, increasing the temperature from 100 to 150 °C significantly reduced the HCOOH formation to levels

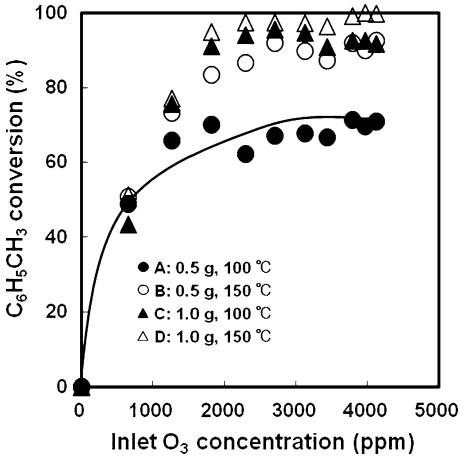

Fig. 4 Toluene conversion over ZSM-5 as a function of inlet O_3 concentration

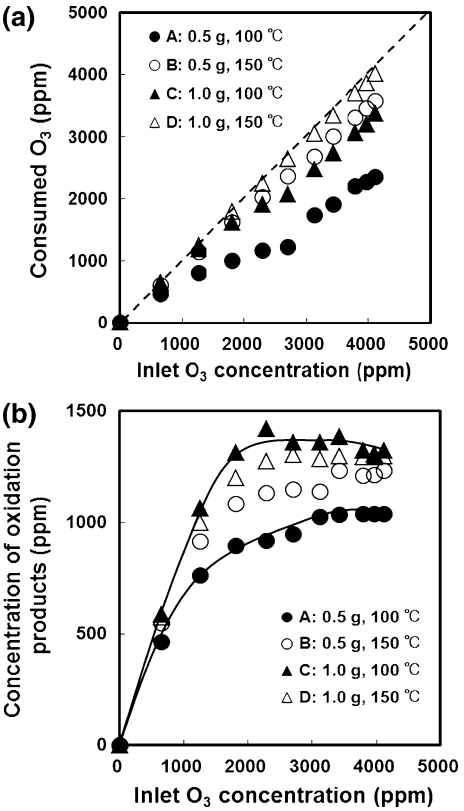

Fig. 5 Influence of reaction conditions on **a** consumed O_3, and **b** concentration of oxidation products. The *dashed line* in **a** shows the values when all the inlet O_3 was consumed. Catalyst: ZSM-5

below 33 and 14 ppm (maximum at 660 ppm O_3) for the conditions of B and D, respectively. When the ozone concentration was higher than 2,700 ppm, no HCOOH was observed at 150 °C. The order of HCOOH formation (A > C > B > D) was inversely proportional to the ozone consumption (Fig. 5) and CO_2 selectivity (D > B > C > A), indicating that the ozone-induced oxygen species on the ZSM-5 surface played an

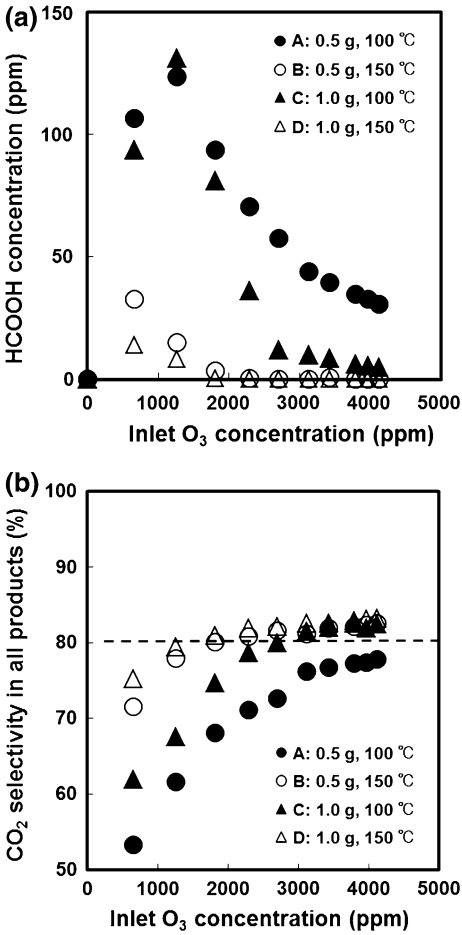

Fig. 6 Influence of reaction conditions on **a** formation of HCOOH, **b** CO_2 selectivity. Catalyst: ZSM-5

important role during the oxidation of toluene. However, the CO_2 selectivity was approximately 83 % at maximum and did not exceed this value, even with 4,000 ppm O_3. These results clearly indicated that the bare ZSM-5 exhibits relatively good activity during initial stage of toluene conversion, but has limited activity in the subsequent steps toward deep oxidation.

Catalytic Activity of Ag/ZSM-5

The toluene conversion over the Ag/ZSM-5 was plotted against the inlet O_3 concentration (Fig. 7). The effects of different reaction conditions (temperature and amount of catalyst) were less significant with the Ag/ZSM-5 than were observed with bare ZSM-5. The maximum conversions were also lower than the conversions observed with the bare ZSM-5. When the inlet O_3 concentration was higher than 2,700 ppm, the toluene conversion became saturated at approximately 70 %, which is about 30 % lower than was observed for the bare ZSM-5 (Fig. 4). Figure 8 shows concentration of the oxidation products and consumed O_3 as functions of the inlet O_3 concentration. As expected from the lower toluene conversion, the Ag/ZSM-5 generated approximately 300 ppm less oxidation

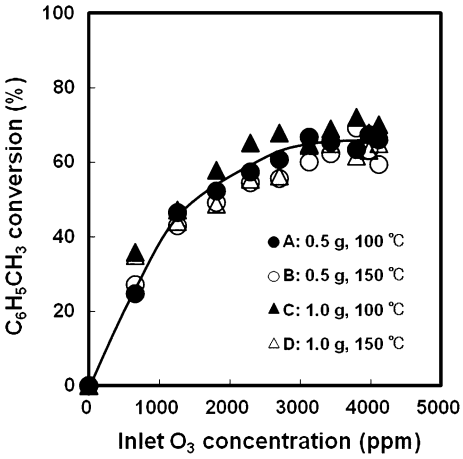

Fig. 7 Toluene conversion over Ag/ZSM-5 as a function of inlet O_3 concentration

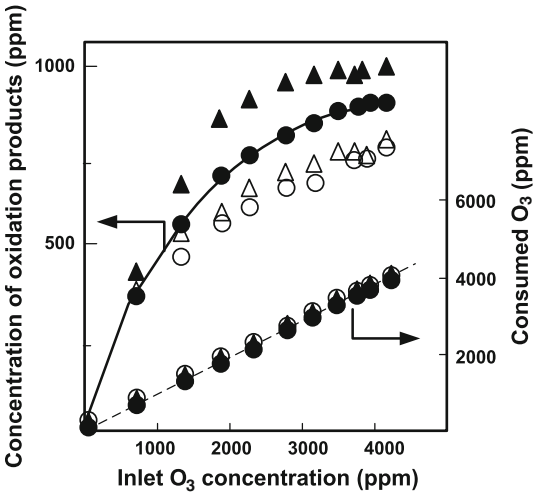

Fig. 8 Concentration of oxidation products and consumed ozone as function of inlet O_3 concentration. Catalyst: Ag/ZSM-5

products by than the bare ZSM-5. However, the Ag/ZSM-5 was effective in the decomposition of ozone. High ozone conversion alongside low toluene conversion indicates that, as will be discussed later (Sect. "Plausible Toluene Oxidation Pathways Over ZSM-5 and Ag/ZSM-5"), facile O_3 consumption occurs over the Ag/ZSM-5. Figure 9 lists the CO_2 selectivities on the Ag/ZSM-5. Regardless of the reaction temperature or amount of catalyst, HCOOH was not formed at all over the Ag/ZSM-5. The CO_2 selectivity was increased under either catalyst amount (0.5 g → 1.0 g) or reaction temperature (100 °C → 150 °C), or both. Under condition D, the CO_2 selectivity reached 99 % at inlet O_3 concentrations higher than 2,300 ppm. Table 1 summarizes effect of the amount of Ag/ZSM-5 on the O_3-assisted catalytic oxidation of 200 ppm toluene at 100 °C. The O_3 consumption increased rapidly with the amount of catalyst, and leveled off when the amount of Ag/ZSM-5 exceeded 0.5 g. These results explain the patterns of consumed O_3 under conditions A, B, C, and D in Fig. 8. The CO_2 selectivities in CO_x were higher than

94 %, regardless of the catalyst amount. For example, toluene conversion with 0.1 g of Ag/ZSM-5 was only 9 % while a 94 % of CO_2 selectivity in CO_x.

Although the Ag/ZSM-5 decomposed O_3 more effectively than the ZSM-5, it was less active during toluene conversion, resulting in fewer amounts of oxidation products. In contrast, the presence of the Ag nanoparticles on ZSM-5 played an important role during the deep oxidation to form CO_2 by reducing the formation of CO and HCOOH. This observation indicates that oxygen species form on the Ag nanoparticles facilitate not only oxidation of toluene and its intermediates but also facile ozone decomposition, leading to much greater ozone consumption without enhancing the oxidation processes.

Oxidations of HCOOH and CO Over the ZSM-5 and Ag/ZSM-5

Oxidation test reactions with HCOOH and CO were performed separately to elucidate the reaction pathways over the ZSM-5 and the Ag/ZSM-5. Table 2 summarizes the HCOOH oxidation with and without O_3 at 100 and 150 °C. The bare ZSM-5 could not oxidize the HCOOH to CO_x at all in the absence of O_3, regardless of reaction temperature. However, the presence of ozone significantly enhanced the HCOOH conversion into CO_2, with an 88 % selectivity. Furthermore, the Ag/ZSM-5 efficiently oxidized 100 ppm of HCOOH to form CO_2 even without O_3 at 100 °C. These results indicate that the two catalysts easily oxidize HCOOH to CO_2 in the presence of O_3. Additionally, the ZSM-5-supported silver nanoparticles played a more important role than the ozone during the oxidation of HCOOH to CO_2.

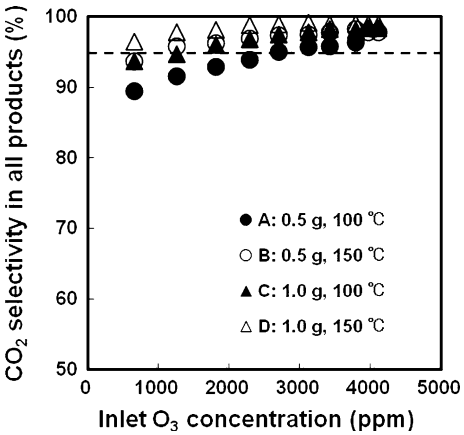

Fig. 9 Relationship between CO_2 selectivity in all products and inlet O_3 concentration. Catalyst: Ag/ZSM-5. The *dashed line* shows the selectivities of 95 %

Table 1 Effect of catalyst amount on toluene oxidation over Ag/ZSM-5 ($[toluene]_0 = 200$ ppm, temperature = 100 °C)

Catalyst amount Ag/ZSM-5 (g)	Supplied O_3 (ppm)	Consumed O_3 (ppm)	$C_6H_5CH_3$ conversion (%)	CO_2 selectivity in CO_x (%)
0.1	2,423	1,074	9	94
0.2	2,423	1,558	23	94
0.5	2,700	2,550	61	95
1.0	2,700	2,677	68	97

Table 2 HCOOH oxidation over ZSM-5 and Ag/ZSM-5 with and without ozone ($[HCOOH]_0 = 100$ ppm, amount of catalyst = 0.5 g)

Catalyst	Reaction temperature (°C)	Supplied O_3 (ppm)	Consumed O_3 (ppm)	HCOOH conversion (%)	CO_2 selectivity in CO_x (%)
ZSM-5	100	–	–	0	–
ZSM-5	150	–	–	0	–
ZSM-5	100	2,423	1,761	100	88
Ag/ZSM-5	100	–	–	97	100
Ag/ZSM-5	100	2,423	2,413	100	100

Table 3 CO oxidation over ZSM-5 and Ag/ZSM-5 with and without ozone ($[CO]_0 = 160$ ppm, amount of catalyst = 0.5 g)

Catalyst	Reaction temperature (°C)	Supplied O_3 (ppm)	Consumed O_3 (ppm)	CO conversion (%)
ZSM-5	100	–	–	0
ZSM-5	150	–	–	0
ZSM-5	100	2,423	1,843	49
ZSM-5	150	2,423	2,112	62
Ag/ZSM-5	100	–	–	48
Ag/ZSM-5	150	–	–	79
Ag/ZSM-5	100	2,423	2,418	100
Ag/ZSM-5	150	2,423	2,423	100

Table 3 depicts the characteristics of the two catalysts during the oxidation of CO under the same conditions as were employed for HCOOH. In the absence of O_3, the bare ZSM-5 could not also oxidize CO at all. The presence of the O_3 promoted CO oxidation to reach 49 and 62 % at 100 and 150 °C, respectively. In contrast, ozone was not necessary for CO oxidation over the Ag/ZSM-5, but it still enhanced the CO oxidation. The Ag/ZSM-5 oxidized 48 and 79 % of CO at 100 and 150 °C, respectively in the absence of O_3. The presence of ozone completely oxidized the CO over the Ag/ZSM-5 at both reaction temperatures. The catalytic activity of Ag on the CO oxidation is consistent with the data reported in literature [47–49]. As shown in Fig. 9, CO_2 selectivity increased with temperature at given amounts of Ag/ZSM-5. This observation indicates that ozone-induced production of surface oxygen species on Ag reacted preferentially with CO and HCOOH rather than toluene.

Plausible Toluene Oxidation Pathways Over ZSM-5 and Ag/ZSM-5

From the above experimental results, plausible steps for the oxidation of toluene with O_3 over ZSM-5 and Ag/ZSM-5 were schematically proposed in Fig. 10. The catalytic effects occurring during an ozone-assisted catalysis are the consequence of the dissociative adsorption of ozone on the surface of the catalyst. Ozone adsorbs onto the active sites of ZSM-5(z) and decomposes to generate active atomic oxygen (z–O*) and O_2 (reactions R1 and R2). Subsequently, z–O* reacts with O_3 to form peroxide (z–O_2*) and desorbs O_2

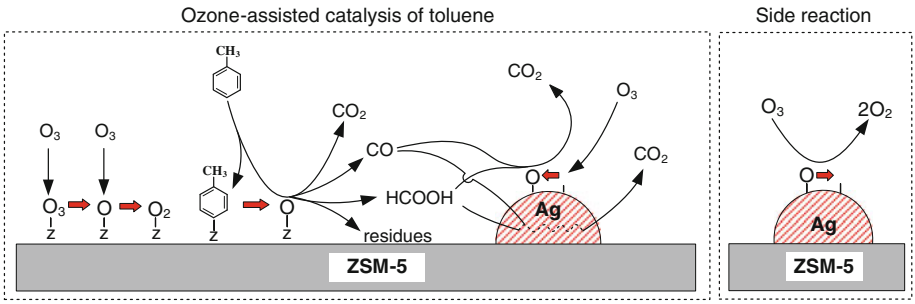

Fig. 10 Plausible reaction pathways of ozone-assisted catalytic oxidation of $C_6H_5CH_3$ over ZSM-5 and Ag/ZSM-5

(reactions R3 and R4) [50]. The higher toluene conversion observed over the bare ZSM-5 indicates that the z–O* is effective in the early steps of toluene decomposition (reactions R5–R7), which is also supported by the enhanced formation of intermediates. However, its ozone-assisted oxidation capacity was limited against these intermediates (HCOOH and CO). No oxidation of HCOOH and CO occurred over the bare ZSM-5 in the absence of O_3 (see Tables 1, 2), which also confirmed that the z–O* plays a key role in the ozone-assisted catalysis of toluene, but does not react with the intermediates over the bare ZSM-5. When the Ag nanoparticles were present on ZSM-5, the deep oxidation of the reaction intermediates was largely enhanced. Ray and Anderegg were most likely the first authors to report an ozone-assisted CO oxidation over Ag [51]. Similar reactions between CO and Ag catalyst have been reported by many authors using various supports such as alumina [42, 52], and NaY [53]. Ozone has a strong interaction with metal surfaces and can induce various surface chemical reactions via ozone-induced surface oxygen species [54]. The surface of metallic Ag (as prepared the Ag/ZSM5) can uptake ozone, which leads to the formation of active oxygen on the surface. Although it is still unclear which of the surface oxygen species (O, O^-, O^{2-}, O_2^-, O_2^{2-}) plays the predominant role in the oxidation process, the presence of a superoxide anion radical (O_2^-) has been confirmed with ESR (electron spin resonance) measurements on the surface of Ag/NaY [53]. Similar observations of ozone-induced oxygen uptake and CO oxidation on Au have been reported by Biener et al. [55].The ZSM-5-supported Ag nanoparticles exhibited some catalytic activity during the oxidations of HCOOH and CO in this study even in the absence of ozone (R12 and R14). The Ag nanoparticles can also catalytically decompose O_3 to O_2, which has been reported by many authors [53, 54, 56]. The Ag–O* in reactions 9 and 10 could be either AgO or Ag_2O. This side reaction (R9) over Ag increases the unproductive consumption of ozone, which does not contribute to the decomposition of either toluene or the intermediates. This result clearly reveals that loading amount of Ag should be carefully designed on the basis of tradeoff between positive effects (R8, R11–R14) and side reaction (R10). One important feature of this figure is that the different reactivity between z–O* and Ag–O*. The z–O* reacts with toluene more efficiently (i.e. R5–R7 > R8), whereas the Ag–O* demonstrates a higher activity against CO and HCOOH oxidation, as well as O_3 decomposition.

$$O_3 + z \rightarrow z{-}O_3 \qquad (R1)$$

$$z{-}O_3 \rightarrow z{-}O^* + O_2 \quad \text{(R2)}$$

$$z{-}O^* + O_3 \rightarrow z{-}O_2 + O_2 \quad \text{(R3)}$$

$$z{-}O_2 \rightarrow z + O_2 \quad \text{(R4)}$$

$$C_6H_5CH_3 + \text{ z-O*} \rightarrow \begin{cases} \text{HCOOH} & \text{(R5)} \\ \text{CO} & \text{(R6)} \\ CO_2 & \text{(R7)} \end{cases}$$

$$C_6H_5CH_3 + Ag{-}O^* \rightarrow \text{Products} \quad \text{(R8)}$$

$$Ag + O_3 \rightarrow Ag{-}O^* + O_2 \quad \text{(R9)}$$

$$Ag{-}O^* + O_3 \rightarrow Ag + 2O_2 \quad \text{(R10)}$$

$$HCOOH + Ag{-}O^* \rightarrow CO_2 \quad \text{(R11)}$$

$$HCOOH + Ag \rightarrow CO_2 \quad \text{(R12)}$$

$$CO + Ag{-}O^* \rightarrow CO_2 \quad \text{(R13)}$$

$$CO + 1/2O_2 + Ag \rightarrow CO_2 \quad \text{(R14)}$$

Ozone-Assisted Catalysis Using Layered Catalysts

To take advantage of the different activities of each catalyst, layered catalysts composed of bare ZSM-5 followed by Ag/ZSM-5 were proposed and tested in the O_3-assisted catalytic oxidation of toluene. Figure 11 summarizes the schematic outline of the layered system, where the two catalysts play slightly different roles in the ozone-assisted decomposition of toluene. Because the bare ZSM-5 exhibits better toluene conversion than the Ag/ZSM-5, it is positioned upstream from the Ag/ZSM-5. The highly ozone-dependent behavior of the bare ZSM-5 also favors the front position. Although less ozone is available in the rear position, the Ag/ZSM-5 catalyst can still efficiently oxidize HCOOH and CO; therefore, the rear position is suitable for the Ag/ZSM-5. Table 4 presents the experimental results of the three sets of layered catalysts alongside the data for the four single catalysts. The layered catalyst achieved both high toluene conversion and high CO_2 selectivity, which was not possible for any of the single catalyst cases. The optimum mixing ratio between the bare ZSM-5 and the Ag/ZSM-5 was found to be an equal amount by mass (0.5 g:0.5 g).

Ozone demand factor (DF_{Ozone}) is a useful measure of how much ozone is necessary during the oxidation of VOC (toluene) [36]. Smaller DF_{ozone}, values correlate with better performance during the ozone-assisted catalysis of toluene.

$$DF_{Ozone} = \frac{\Delta[O]_3}{\Delta[\text{Toluene}]} = \frac{\Delta[O]_3}{([CO]_2 + [CO] + [CHOOH])/7} \quad (3)$$

When drawing comparisons based on DF_{ozone}, a good carbon balance (Δ[toluene] = sum of products) is necessary to make a reasonable evaluation.

$$C_6H_5CH_3 + 18O_3 \rightarrow 7CO_2 + 4H_2O + 18O_2 \quad \text{(R15)}$$

The stoichiometric DF_{ozone} for the reaction between toluene and ozone (R15) is 18. This value ($DF_{ozone} = 18$) means that ozone provides an equi-molar amount of atomic oxygen

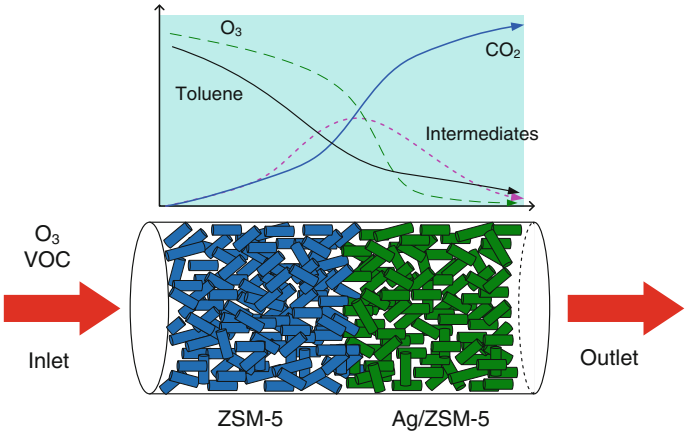

Fig. 11 Functionalized two-layer catalysts for ozone-assisted catalysis of toluene

Table 4 Toluene oxidation over layered catalyst (ZSM-5 and Ag/ZSM-5) ([toluene]$_0$ = 200 ppm, temperature = 100 °C)

Catalyst		Supplied O_3 (ppm)	Consumed O_3 (ppm)	$C_6H_5CH_3$ conversion (%)	HCOOH concentration (ppm)	Carbon balance (%)	CO_2 selectivity in all products (%)	DF_{Ozone}
ZSM-5	Ag/ZSM-5							
0.5	–	2,700	1,222	67	58	122	73	9.1
1.0	–	2,700	2,067	96	12	102	80	10.7
–	0.5	2,700	2,550	61	0	104	95	20.9
–	1.0	2,700	2,677	68	0	128	97	19.6
0.9	0.1	2,423	2,087	86	23	97	83	12.1
0.8	0.2	2,423	2,153	86	11	100	86	12.5
0.5	0.5	2,700	2,591	91	0	100	94	14.2

to the reaction before it reforms oxygen. With the single catalysts, the DF_{ozone} values for the bare ZSM-5 and the Ag/ZSM-5 were approximately 10 and 20, respectively. In the two-layered cases, the DF_{ozone} increased with the Ag/ZSM-5 amount from 12.1 to 14.2, which is most likely due to the side reactions (R9) and (R10) occurring over Ag. From the work by Kwong et al. [38], the DF_{ozone} for the removal of 1.5 ppmv toluene at room temperature had an estimated range of 20–35. More work is necessary (the effects of initial condition, type of catalyst, and temperature) to optimize the DF_{ozone} value, which is also related to the process economy.

Conclusion

In this study, the different behaviors of the bare ZSM-5 versus the Ag/ZSM-5 during the ozone-assisted catalytic degradation of toluene were clarified. The bare ZSM-5 had higher activity during the toluene conversion, but not for the oxidation process that formed CO_2. The Ag/ZSM-5 displayed less efficient toluene conversion, but it had higher activity during

the oxidation of intermediates (HCOOH and CO). The DF_{Ozone}, indicated that the Ag/ZSM-5 consumed more ozone because ozone undergoes catalytic decomposition over Ag nanoparticles. We incorporated two different catalysts with complementary activities into a layered system to enhance both the toluene conversion and the CO_2 selectivity. A layered catalyst constructed with equal amounts of bare ZSM-5 and Ag/ZSM-5 could achieve high toluene conversion in addition to an oxidation to form CO_2, which was impossible when using either catalyst singly. The layered catalyst incorporates different catalytic activities, which may lead to the development of systems less dependent on the amount of precious metal; generating these types of catalysts may also lead to reduced process costs.

Acknowledgments This work was partially supported by the Environmental Technology Development Fund (S2-01) from the Ministry of the Environment, Japan.

References

1. Everaert K, Baeyens J (2004) J Hazard Mater B109:113–139
2. Spivey JJ (1987) Ind Eng Chem Res 26:2165–2180
3. Cooper CD, Alley FC (2002) Air pollution control: a design approach, 3rd edn. Waveland Press Inc, Long Grove, pp 321–458
4. Zhao X, Yin M, Ma L, Liang L, Liu C, Liao J, Lu T, Xing W (2011) Energy Environ Sci 4:2525–2529
5. Li X, Wang L, Xia Q, Liu Z, Li Z (2011) Catal Commun 14:15–19
6. Nanba T, Masukawa S, Uchisawa J, Obuchi A (2008) J Catal 259:250–259
7. Chen HL, Lee HM, Chen SH, Chang MB, Yu SJ, Li SN (2009) Environ Sci Technol 43:2216–2227
8. Vandenbroucke AM, Morent R, Geyter ND, Leys C (2011) J Hazard Mater 195:30–54
9. Kim HH, Ogata A (2011) Eur Phys J Appl Phys 55:13806
10. Kim HH, Takashima K, Katsura S, Mizuno A (2001) J Phys D Appl Phys 34:604–613
11. Holzer F, Roland U, Kopinke F-D (2002) Appl Catal B: Environ 38:163–181
12. Dimitrova S, Ivanov G, Mehandjiev D (2004) Appl Catal A: Gen 266:81–87
13. Konova P, Stoyanova M, Naydenov A, Christoskova S, Mehandjiev D (2006) Appl Catal A: Gen 298:109–114
14. Gervasini A, Vezzoli G, Ragaini V (1996) Catal Today 29:449–455
15. Yamamoto T (1999) J Hazard Mater B67:165–181
16. Futamura S, Zhang Z, Yamamoto T (1999) IEEE Trans Ind Appl 35(4):760–766
17. Marotta E, Paradisi C (2005) J Mass Spectrom 40:1583–1589
18. Ono R, Nakagawa Y, Oda T (2011) J Phys D Appl Phys 44:485201
19. Guaitella O, Gatilova L, Rousseau A (2005) Appl Phys Lett 86:151502
20. Blin-Simiand N, Pasquiers S, Jorand F, Postel C, Vacher JR (2009) J Phys D Appl Phys 42:122003
21. Ono R, Tobaru C, Teramoto Y, Oda T (2009) Plasma Sour Sci Technol 18(2):025006
22. Kim HH, Hwang N, Ogata A, Song YH (2011) IEEE Trans Plasma Sci 39(11):2220–2221
23. Kim HH, Kim JH, Ogata A (2009) J Phys D Appl Phys 42:135210
24. Ogata A, Yamanouchi K, Mizuno K, Kushiyama S, Yamamoto T (1999) IEEE Trans Ind Appl 35(6):1289–1295
25. Ogata A, Ito D, Mizuno K, Kushiyama S, Yamamoto T (2001) IEEE Trans Ind Appl 37(4):959–964
26. Holzer F, Kopinke FD, Roland U (2005) Plasma Chem Plasma Proc 25(6):595–611
27. Harling A, Glover DJ, Whitehead JC, Zhang K (2009) Appl Catal B: Environ 90:157–161
28. Sekiguchi K, Sanada A, Sakamoto K (2003) Catal Commun 4:247–252
29. Einaga H, Futamura S (2006) J Catal 243:446–450
30. Zhao DZ, Shi C, Li XS, Zhu AM, Jang BWL (2012) J Hazard Mater 239:362–369
31. Rezaei E, Soltan J (2012) Chem Eng J 198–199:482–490
32. Xi Y, Reed C, Lee YK, Oyama ST (2005) J Phys Chem B 109:17587–17595
33. Long L, Zhao J, Yang L, Fu M, Wu J, Huang B, Ye D (2011) Chin. J Catal 32:904–916
34. Almquist CB, Sahle-Demessie E, Sehker SC, Sowash J (2007) Environ Sci Technol 41(13):4754–4760
35. Kastner JR, Buquoi Q, Ganagavaram R, Das KC (2005) Environ Sci Technol 39:1835–1842
36. Ogata A, Saito K, Kim HH, Sugasawa M, Aritani H, Einaga H (2010) Plasma Chem Plasma Proc 30:33–42
37. Gervasini A, Ragaini V (2000) Catal Today 60:129–138

38. Kwong CW, Chao CYH, Hui KS, Wan MP (2008) Environ Sci Technol 42(22):8504–8509
39. Kwong CW, Chao CYH, Hui KS, Wan MP (2008) Atmospheric Environ 42:2300–2311
40. Sugasawa M, Ogata A (2011) Ozone Sci Eng 33:158–163
41. Einaga H, Futamura S (2004) J Catal 227:304–312
42. Einaga H, Futamura S (2004) React Kinet Catal Lett 81(1):121–128
43. Kim HH, Ogata A, Futamura S (2006) IEEE Trans Plasma Sci 34(3):984–995
44. Li W, Gibbs GV, Oyama ST (1998) J Am Chem Soc 120:9041–9046
45. Li W, Oyama ST (1998) J Am Chem Soc 120:9047–9052
46. Reed C, Xi Y, Oyama ST (2005) J Catal 235:378–392
47. Burghaus U, Conrad H (1996) Surf Sci 352:253–257
48. Kang Y, Sun M, Li A (2012) Catal Lett 142:1498–1504
49. Biabani-Ravandi A, Rezaei M, Fattah Z (2013) Chem Eng J 219:124–130
50. Chao CYH, Kwong CW, Hui KS (2007) J Hazard Mater 143:118–127
51. Ray AB, Anderegg FO (1921) J Am Chem Soc 43(5):967–978
52. Einaga H, Ogata A (2010) Environ Sci Technol 44(7):2612–2617
53. Imamura S, Ikebata M, Ito T, Ogita T (1991) Ind Eng Chem Res 30:217–221
54. Dhandapani B, Oyama ST (1997) Appl Catal B: Environ 11:129–166
55. Biener J, Wittstock A, Zepeda-Ruiz LA, Biener MM, Zielasek V, Kramer D, Viswanath RN, Weissmüller J, Bäumer M, Hamza AV (2009) Nat Mater 8:47–51
56. Kumar N, Konova PM, Naydenov A, Heikillä T (2004) Catal Lett 98(1):57–60